Comparative Phosphoproteomics Reveals Components of Host Cell Invasion and Post-transcriptional Regulation During *Francisella* Infection*[S]

Ernesto S. Nakayasu‡§§‡‡, Rebecca Tempel§§§, Xiaolu A. Cambronne¶, Vladislav A. Petyuk‡, Marcus B. Jones‖, Marina A. Gritsenko‡, Matthew E. Monroe‡, Feng Yang‡, Richard D. Smith‡, Joshua N. Adkins‡, and Fred Heffron§**

Francisella tularensis* is a facultative intracellular bacterium that causes the deadly disease tularemia. Most evidence suggests that *Francisella* is not well recognized by the innate immune system that normally leads to cytokine expression and cell death. In previous work, we identified new bacterial factors that were hyper-cytotoxic to macrophages. Four of the identified hyper-cytotoxic strains (*lpcC, manB, manC*, and *kdtA*) had an impaired lipopolysaccharide (LPS) synthesis and produced an exposed lipid A lacking the O-antigen. These mutants were not only hyper-cytotoxic but also were phagocytosed at much higher rates compared with the wild type parent strain. To elucidate the cellular signaling underlying this enhanced phagocytosis and cell death, we performed a large-scale comparative phosphoproteomic analysis of cells infected with wild-type and *delta-lpcC F. novicida*. Our data suggest that not only actin but also intermediate filaments and microtubules are important for *F. novicida* entry into the host cells. In addition, we observed differential phosphorylation of tristetraprolin, a key component of the mRNA-degrading machinery that controls the expression of a variety of genes including many cytokines. Infection with the *delta-lpcC* mutant induced the hyper-phosphorylation and inhibition of tristetraprolin, leading to the production of cytokines such as IL-1beta and TNF-alpha that may kill the host cells by triggering apoptosis. Together, our data provide new insights for *Francisella* invasion and a post-transcriptional mechanism that prevents the expression of host immune response factors that control infection by this pathogen. *Molecular & Cellular Proteomics 12: 10.1074/mcp.M113.029850, 3297–3309, 2013.

Francisella tularensis is the Gram-negative facultative intracellular bacterium that causes the disease tularemia in humans and diverse animals. This bacterium is among the most virulent human pathogens known, with inhalation or inoculation of as few as 10 bacteria being sufficient to cause a fatal infection. Its low infectious dose and relative ease of airborne transmission led to the development of *F. tularensis* as a biological weapon (1). Because of potential threats to national security and public health, the U.S. Centers for Disease Control and Prevention (CDC) classifies *F. tularensis* as a Category A bioterrorism agent, and the Departments of Health and Human Services (HHS) and Agriculture (USDA) list this pathogen as a Tier 1 select agent. (http://www.bt.cdc.gov/agent/agentlist-category.asp; http://www.selectagents.gov/select%20agents%20and%20toxins%20list.html).

Francisella tularensis includes three subspecies: *tularensis* (abbreviated as *F. tularensis*), *holarctica* (abbreviated as *F. holarctica*), and *mediasiatica* (abbreviated as *F. mediasiatica*) (2). Of these, *F. tularensis* subsp. *tularensis* and subsp. *holarctica* are capable of causing disease in humans and must be manipulated in a Biosafety Level 3 environment. *Francisella novicida* (abbreviated as *F. novicida*) is a closely related species to *F. tularensis* and shares high genetic similarity to other *F. tularensis* subspecies (~98% DNA sequence identity) (3, 4). Although some differences have been observed so far between *F. novicida* and *F. tularensis*, mainly in their lipopolysaccharide (LPS)[1] O-antigen and the ability to activate the inflammasome, most of the mutations in orthologous genes generate similar phenotypes (5–7). Because of the avirulence in humans for the U112 isolate (8) and ability to cause a

From the ‡Biological Science Division, Pacific Northwest National Laboratory, Richland, Washington; §Department of Molecular Microbiology and Immunology, Oregon Health and Science University, Portland, Oregon; ¶Vollum Institute, Oregon Health and Science University, Portland, Oregon; ‖Pathogen Functional Genomics Resource Center, J. Craig Venter Institute, Rockville, Maryland

Received April 5, 2013, and in revised form, August 15, 2013
Published, MCP Papers in Press, August 22, 2013, DOI 10.1074/mcp.M113.029850

[1] The abbreviations used are: LPS, lipopolysaccharide; ASC, apoptosis-associated speck-like protein containing a caspase recruitment domain; CDC, Centers for Disease Control and Prevention; CR3, CR3 complement receptor; CytD, cytochalasin D; (FcγR), Fc-gamma receptor; iTRAQ, isobaric tags for relative and absolute quantification; MAPK, mitogen-activated protein kinase; MR, mannose receptor; SEN, surface-exposed nucleolin; SRA, scavenger receptor A; TLR, toll-like receptor; TTP, tristetraprolin; WT, wild-type.

tularemia-like disease in animal models, *F. novicida* provides a safe and appropriate research alternative to virulent *F. tularensis* strains.

Although research efforts have elucidated many of the molecular mechanisms of *Francisella* pathogenesis over the past decade (9–12), the detailed mechanistic interplay between bacterial factors and the host immune response remains incomplete. One of the first steps during the bacteria-host interaction is the phagocytosis or entry of bacteria into the host cells. To date, there are five receptors described in the phagocytosis of *Francisella* by macrophages: scavenger receptor A (SRA), mannose receptor (MR), Fc-gamma receptor (FcγR), CR3 complement receptor (CR3) and surface-exposed nucleolin (SEN) (13–16). After being recognized by one of these receptors *Francisella* triggers a signaling cascade that culminates in the rearrangement of actin filaments and engulfment of the bacteria (17–19). This signaling cascade is in part regulated by phosphorylation and dependent on kinases such as Akt, Syk and Erk (20, 21). More recently, *Francisella* was also shown to be endocytosed by liver cells in a mechanism that involved cholesterol-rich domains on the plasma membrane and clathrin-coated vesicles (22). In addition to phagocytosis, the host inflammatory response through TLR signaling and the activation of the inflammasome are also essential factors during the early stages of the infection (9–11, 23).

Francisella has quite a distinct inflammatory response compared with other Gram-negative bacteria. Unlike *E. coli* or *Salmonella*, the lipopolysaccharide (LPS) from *Francisella* is not endotoxic and lacks the ability to stimulate toll-like receptor 4 (TLR4), the pro-inflammatory receptor that recognizes Gram-negative bacteria (24). The lack of TLR4 activation is related to hypoacylation and the addition of very long chain fatty acids to the diglucosamine backbone of the lipid A portion of LPS (24). Typically, TLR4 is activated by lipid A containing six short (12–14 carbon) fatty acids, whereas *Francisella* lipid A has four fatty acids with longer carbon chains (16–18 carbon) (11, 24). On the other hand, *Francisella* has been shown to activate TLR2 (25, 26) that recognizes lipoproteins, glycans, and glycophospholipids more frequently present in Gram-positive bacteria, fungi, and protozoan parasites, respectively (27). *Francisella* also activates another component of innate immune system—the inflammasome (10). Assembly of the inflammasome is activated by *Francisella* infection and is responsible for triggering a pro-inflammatory response through processing and maturing cytokines, such as IL-1β and IL-18 (28–32), in addition to triggering a pro-inflammatory response that leads to cell death by pyroptosis (30–33). More recently, Peng *et al.* showed that several *Francisella* mutants defective in membrane proteins were hyper-cytotoxic to host cells in a process that is dependent on the inflammasome (29).

It has been proposed that *Francisella* actively suppresses signaling by TLRs and the inflammasome to evade the host immune system and effectively establish an infection (11). To identify genes that are involved in host immune evasion, we recently screened a comprehensive mutant library containing over 3000 *F. novicida* strains for mutants that were hyper-cytotoxic (34). Among the identified strains four *F. novicida* genes were involved in LPS core synthesis and assembly. These mutants are unable to synthesize the LPS core and thus produce LPS with a very short glycan compared with the long polysaccharide chains of the wild-type (WT) (34). Interestingly, three mutants (Δ*lpcC*, Δ*manB*, and Δ*manC*) are hyper-cytotoxic to RAW 264.7 cells, a murine macrophage-like cell line that lacks the production of ASC (apoptosis-associated speck-like protein containing a caspase recruiting domain), a key component of the inflammasome signaling. This observation suggests that although Δ*lpcC*, Δ*manB*, and Δ*manC* are also defective in membrane components, the mechanism of cell killing may be different than the mutant strains studied by Peng *et al.* (29). Also surprising was that Δ*lpcC*, Δ*manB*, and Δ*manC* strains were phagocytosed at a much higher rate than WT *F. novicida* via a mechanism that does not require actin polymerization (34). Actin polymerization has thus far been demonstrated to be involved in internalization of *Francisella* by either phagocytic or endocytic pathways (21, 22, 35); therefore, the finding that Δ*lpcC*, Δ*manB*, and Δ*manC* mutant strains are able to invade host cells independent of actin filaments remains to be understood. Deletion of *lpcC* from *F. tularensis* Schu S4 also results in a similar phenotype, suggesting that this phenomenon acts broadly among the different *Francisella* species rather than specific to *F. novicida* (Tempel and Heffron, unpublished observations).

To better understand the mechanism of infection and cell killing by these hyper-cytotoxic *F. novicida* strains, we evaluated cell signaling stimulated by the *F. novicida* Δ*lpcC* strain in comparison to its parent WT strain. Here we carried out a comprehensive quantitative phosphoproteomic analysis using isobaric tags for relative and absolute quantification (iTRAQ), which allowed us to analyze WT and Δ*lpcC F. novicida* infection with multiple replicates in the same experiment. By combining network and function-enrichment analyses followed by immunological and cellular experiments we identified new mechanistic aspects of host phagocytosis and cell killing by *F. novicida*.

EXPERIMENTAL PROCEDURES

Ethics Statement—Mouse experiments were approved under the protocol of the Oregon Health and Science University Institutional Animal Care and Use Committee (IACUC B11220) and performed in accordance with the guidelines for the Care and Use of Laboratory Animals of the National Institutes of Health to minimize animal suffering.

Bacterial Culture—Wild type and Δ*lpcC Francisella novicida* were grown on cysteine heart agar (CHA) from −80 °C freezer stocks before culturing in liquid media. Bacteria were cultured overnight in tryptic soy broth + 0.1% cysteine (TSBC) with shaking (200 rpm), and

the optical density at 600 nm (OD_{600}) was measured to determine CFU/ml.

Cell Culture and Infection—RAW 264.7 or J774 murine macrophage-like cells (American Type Culture Collection, Manassas, VA) were cultured in DMEM/High Glucose (HyClone, Logan, UT) supplemented with 10% fetal bovine serum (FBS; Invitrogen, Rockville, MD) at 37°C in the presence of 5% CO_2. For infection, bacteria were added to 50–80% confluent cells in tissue culture plates at a multiplicity of infection (MOI) of 100. The cells were centrifuged at 1000 × *g* for 5 min at room temperature and incubated at 37°C with 5% CO_2. Thirty minutes to 1 h after infection, cells were washed three times with PBS and either prepared for analysis (time = 0) or overlaid with DMEM containing 100 μg/ml gentamicin to prevent growth of extracellular bacteria and incubated at 37°C with 5% CO_2. After one hour, cells were washed three times with PBS and either prepared for analysis or overlaid with 10 μg/ml gentamicin and incubated at 37°C with 5% CO_2 for the duration of the infection. Each infection assay is performed in triplicate unless otherwise stated.

Western Blot Analysis—RAW 264.7 or J774 murine macrophage-like cell lines were cultured as described in 6-well plates and either subjected to mock infections or acute 1 h infections with wild-type (U112) or Δ*lpcC F. novicida* strains, as indicated. Following infection, cells were washed three times in PBS and incubated with media containing 100 nM okadaic acid and 10 μg/ml gentamycin. Four hours after initial exposure to *Francisella*, cells were collected in PBS and pellets stored at −80°C for 10 min. Cell pellets were then lysed in the presence or absence of phosphatase inhibitors and EDTA depending on whether they were to undergo lambda phosphatase treatment (20 mM Tris pH7.4, 150 mM NaCl, 0.5% Nonidet P-40, 1 mM dithiothreitol (DTT), protease inhibitor mixture (Roche), ± 5 mM EDTA, ± 10 mM NaF, ± 10 mM Na_3VO_4, ± 10 mM p-Nitrophenyl phosphate, ± 100 nM Okadaic Acid, and ± 1× HALT phosphatase inhibitor mixture (Pierce, Rockford, IL)). Thirty μg of cleared whole cell lysates (quantified using the Bradford assay) was resolved on 10% Tris-Glycine SDS-PAGE. Manganese and 5 U of lambda phosphatase (New England Biolabs, Ipswich, MA) were added to whole cell lysates as indicated and the reaction was incubated at 30°C for 30 min; stopped with Laemmli protein loading buffer. Transferred proteins were subjected to Western blot analysis using anti-TTP 1:1000 (Millipore ABE285), anti-RNA Pol II Rpb1 1:1000 (SCBT sc-900), and anti-rabbit IgG-HRP secondary 1:10,000 (Promega, Madison, WI).

Cytokine Assay—RAW 264.7 cells were infected in triplicate with Δ*lpcC*, parent, mock, or untreated in 24-well plates as described above for 0, 2, or 6 h. At the end of each time point, 350 μl of supernatant was frozen at −80°C and submitted for analysis. The samples were tested on Quansys Biosciences' (Logan, UT) Q-Plex Array™ kits for expression of 21 unique cytokines. Q-Plex™ technology is a multiplex approach that involves the micro-spotting of individual groups of capture antibody in either a Cartesian or polar coordinate system on the bottom of a 96-well plate, each spot being its own micro ELISA. Each well was identically spotted. Standard ELISA procedures were applied notably initial sample incubation, washing, secondary antibody incubation, washing, incubation with the label, and measurement are involved. The label and reporting system used in a Q-Plex Array™ is chemiluminescent.

Apoptosis and Necrosis Assay—RAW 264.7 cells were infected for 18 h in triplicate in an opaque white 96-well tissue culture plate (BD, Billerica, MA) with Δ*lpcC*, WT U112, mock, or uninfected. 10 mM staurosporine or 100 mM ionomycin were added to triplicate wells as controls for apoptosis or necrosis, respectively. Thirty minutes before analysis, 5 μl of 10% saponin was added to triplicate control wells as a lysis control. The cells were analyzed for viability, cytotoxicity, and apoptosis using the ApoTox-Glo™ Triplex Assay (Promega) according to manufacturer's instructions. The assay was read using a SpectraMax® Gemini™ XS plate reader (Molecular Devices, Sunnyvale, CA).

Cytotoxicity (Cell Invasion) Assay—J774 cells were infected in triplicate in 24-well tissue culture plates (BD, Billerica, MA) with Δ*lpcC*, WT, mock, or uninfected, ± cells invasion inhibitors (cytochalasin D, 5 μg/ml; nocodazole, 10 μg/ml; withaferin A, 5 μM; wortmannin, 0.1 μM). One hour after infection, the cells were washed and incubated with DMEM containing 100 μg/ml gentamicin, as above. After one hour of incubation with gentamicin, macrophages were washed and lysed with 0.5% saponin for 30 min at 37°C, and the lysates were serially diluted and plated on CHA plates to determine *F. novicida* CFU/ml.

Protein Extraction and Trypsin Digestion—In preparation for phosphorylation analyses, RAW 264.7 macrophage-like cells were infected with either wild-type or Δ*lpcC Francisella* strains as described above for 30 min, washed with PBS and incubated for an additional 0, 1, 2, and 4 h. The contents of each well of the 6-well plates were resuspended in 500 μl of lysis buffer (8 M urea in 100 mM NH_4HCO_3 pH 8.0 containing Sigma phosphatase inhibitor cocktails 1 and 3). The contents of 3 wells were combined and stored at −80°C. Proteins were then thawed and quantified by BCA assay (Pierce). Protein disulfide bonds were reduced by DTT (5 mM) for 1 h at 37°C, and the resulting free thiol groups were alkylated by iodoacetamide (20 mM) for 1 h at room temperature in the dark. After alkylation, samples were diluted 4-fold with 50 mM NH_4HCO_3 (pH 7.8) and digested with trypsin at ratio of 1:50 (trypsin/protein) for 4 h at 37°C, diluted by another 2-fold with the same buffer, and subjected to a second treatment with trypsin and incubated at room temperature overnight. The reaction was stopped by lowering the pH to 2.5 with trifluoroacetic acid. The resulting peptides were desalted using C18 SPE (Discovery DSC-18, Supelco) cartridges, concentrated down in SpeedVac SC250 Epress (ThermoSavant) and their concentrations were measured by BCA assay.

iTRAQ Labeling and Phosphopeptide Enrichment—Peptides (50 μg) from each sample were subjected to 8-plex iTRAQ (Applied Biosystems) labeling as the experimental design in Fig. 1, and according to the manufacturer recommendations. Each iTRAQ experiment had biological duplicate controls with mock infections and biological triplicates of RAW 264.7 cells infected with either wild-type or Δ*lpcC F. novicida* strains, all collected at the same time point. After labeling and mixing equal amounts of peptides, samples were desalted using C18 SPE cartridges, concentrated in a SpeedVac and submitted to quantification by BCA assay. The phosphopeptide enrichment was performed exactly as described by Nguyen *et al.*, using Fe^{3+}-nitriloacetic acid functionalized magnetic beads (36). After enrichment, phosphopeptides were concentrated by vacuum centrifugation before mass spectrometry analysis.

Proteomic Analysis—Phosphopeptides were loaded to a trap column (150 μm i.d. × 4 cm; 5 μm C18 particles, Phenomenex) and the separation was achieved in a longer column (50 μm i.d. × 40 cm; 5 μm C18 particles, Phenomenex) using an isobaric gradient of acetonitrile over 200 min (37). Eluted peptides were directly analyzed by electrospray ionization - mass spectrometer (Orbitrap Velos equipped with ETD). Full scan - 400–200 *m/z* with resolution of 60,000 at 400 *m/z*. The five most intense ions were selected for HCD (40% normalized collision energy) followed by decision tree ETD ($z = 3$, $m/z<650$; $z = 4$, $m/z<900$; $z = 5$, $m/z<950$) or CID scans ($z = 2$; $z = 3$, $m/z>650$; $z = 4$, $m/z>900$; $z = 5$, $m/z>950$). MS/MS spectra were converted to peak lists using DeconMSn (version 2.2.2.2, http://omics.pnl.gov/software/DeconMSn.php) (38) using default parameters and database searched using SEQUEST v27 against murine protein sequences from Uniprot (downloaded on August 22nd, 2011) and porcine trypsin both in forward and reverse orientations (32,780 total sequences). As searching parameters, precursor ion mass tol-

erance was 50 ppm, and fragmentation tolerances for CID, ETD, and HCD were 0.5, 0.5, and 0.05 Da, respectively. Only fully tryptic peptides were considered, with two missed cleavages allowed. Phosphorylation (+79.9663 Da) of serine, threonine, or tyrosine was searched as a dynamic modification. Cysteine carbamidomethylation (+57.0215 Da) and lysine and N terminus labeling with iTRAQ (+304.2022 Da) were searched as static modifications. The maximum number of variable modifications was set to 3. Peptides were then filtered using a cutoff of MSGF (39) ≤ 1.0e-9, which resulted in ~1% false-discovery rate. When peptides matched multiple sequences only the first in the database was reported. Ascore (40) was used to estimate the confidence of phosphorylation modification site assignment, Sites with an A-Score ≥ 19 were considered as unambiguous sites (≥ 99% confidence). Sites with −1 Ascore indicate these sites are the only choices for modification on the peptide identified.

Quantitative Data Analysis—iTRAQ reporter ion intensities were extracted with MASIC (MS/MS Automated Selected Ion Chromatogram Generator, version v2.5.3923, http://omics.pnl.gov/software/MASIC.php) (41) and the phosphopeptides fragmented multiple times were summed together to remove redundancy in quantification and improve signal to noise ratio followed by log transformation. To convert $\log_2$ (ion intensities) to relative abundance measures we subtracted the mean log intensity values for each individual peptide. The normalization step was based on assumption that the majority of phosphopeptides do not change in one direction, and the median relative abundance should be equal between samples. This type of normalization allows removing biases arising from pipetting error or labeling efficiency. The missing data was imputed using K-NN approach similar to described previously (42), using Spearman correlation as a distance measure. Because of the low number of replicates (2–3), for testing of statistical significance of differential abundance of phosphopeptides we applied a moderated ANOVA test available in the "limma" BioConductor package (43). Pairwise differences were inferred by applying post-hoc contrasts analysis (Mock-WT, Mock-Δ*lpcC*, WT-Δ*lpcC*). The significance threshold was set at 0.05 of Benjamin-Hochberg adjusted *p* value. All of the time points (0, 1, 2 and 4 h) were analyzed independently.

Sequence Analysis—Motif analysis for specific kinases was performed online using motif-x (http://motif-x.med.harvard.edu/motif-x.html) (44). For this analysis only confident phosphorylation sites with Ascore ≥ 19.0 or –1 were used, and results were filtered with an enrichment significance ≤ 0.01. The number of occurrences was adjusted to 5 or 10 depending on the number of queried phosphosites. The protein-protein interaction network was built based on the information deposited at InnateDB (innatebd.org, updated February 16th, 2012) (45). Proteins from experimentally verified interactions were retrieved from InnateDB and the network was built in Cytoscape v2.8.3 (cytoscape.org) (46). After building the network, only proteins that directly interact with at least 2 phosphoproteins were kept. The function-enrichment analysis was performed online using the Database for Annotation, Visualization and Integrated Discovery (DAVID) v6.7 (http://david.abcc.ncifcrf.gov/home.jsp) (47).

Murine Infection—Four- to six-week-old female C57BL/6J mice were purchased from Jackson Laboratories (Bar Harbor, Maine) and allowed to acclimatize for 1 week before infection. Groups of three mice were infected intraperitoneally (intraperitoneal) with 2×10^4 CFU of WT or Δ*lpcC F. novicida*, mock infected with PBS, or left untreated. At 48 h postinfection, whole spleens were harvested, cut into 3 pieces and placed in RNAlater (Ambion) at 4°C overnight before storing at −80°C. All procedures and protocols were performed at OHSU in compliance with Institutional Animal Care and Usage Committee guidelines.

Generation of Probes for Microarray Experiments—DNA probes for microarray experiments were generated by adding 2 μg of total RNA in a mixture containing 6 μg of random hexamers (Invitrogen), 0.01 M dithiothreitol, an aminoallyl-deoxynucleoside triphosphate mixture containing 25 mM each dATP, dCTP, and dGTP, 15 mM dTTP, and 10 mM amino-allyl-dUTP (aa-dUTP) (Sigma), reaction buffer, and 400 units of SuperScript III reverse transcriptase (Invitrogen) and incubating at 42°C overnight. The RNA template then was hydrolyzed by adding NaOH and EDTA to a final concentration of 0.2 and 0.1 M, respectively, and incubating at 70°C for 15 min. Unincorporated aa-dUTP was removed with a QIAquick column (Qiagen). The probe was eluted with phosphate elution buffer (4 mM KH_2PO_4, pH 8.5, in ultrapure water), dried, and resuspended in 0.1 M sodium carbonate buffer (pH 9.0). To couple the amino-allyl cDNA with fluorescent labels, Cy3 or Cy5 (Amersham Biosciences) was added for 1h. Uncoupled label was removed using the Qiagen QIAquick PCR purification kit (Valencia, CA).

Microarray Hybridization, Scanning, Image Analysis, Normalization, and Analysis—Agilent 4 × 44K mouse gene expression arrays were used. Hybridization protocol was performed by manufacturer's suggestion. Equal volumes of the appropriate Cy3- and Cy5-labeled probes were combined, dried, and then resuspended in the hybridization buffer and were heated to 95°C before hybridization. The probe mixture then was added to the microarray slide and allowed to hybridize overnight at 42°C with rotation in the Agilent hybridization oven. Hybridized slides were washed sequentially in Agilent wash buffer #1 and wash buffer #2. Individual TIFF images from each channel were captured and analyzed with Agilent Feature Extractor. Microarray data were normalized by LOWESS in TIGR MIDAS software (available at http://www.jcvi.org/software/tm4) and data visualized in TMEV.

mRNA Stability Assay—RAW 264.7 macrophage-like cells were infected with either wild-type or Δ*lpcC Francisella* strains in biological triplicate for 1 h, followed by washes and addition of gentamicin as described above. Cells were then treated with Actinomycin D (5 μg/ml) and indicated time points were harvested directly in Trizol (Invitrogen). From each replicate and time point, 500 ng of purified total RNA was used for cDNA synthesis using oligoDT primers. Quantitative PCR was performed using gene-specific primers for rRNA 18S, Gapdh, IL-1β, and RANTES transcripts. (IL-1β: TTGACAGTGATGAGAATGACCTG, GAGATTTGAAGCTGGATGCTCT; RANTES: TTGCAGTCGTGTTTGTCACTC, TTCTTGAACCCACTTCTTCTCTG). Values were normalized to rRNA 18S transcript as well as relative to their baseline abundance at time 0.

RESULTS AND DISCUSSION

Changes in Host Cell Phosphoproteome Induced by F. novicida *Infection*—In an effort to identify pathways that are activated during cell invasion by *Francisella* we performed a quantitative phosphoproteomic analysis of RAW 264.7 macrophage-like cells infected with either wild-type or Δ*lpcC Francisella* strains. A total of 3008 phosphopeptides from 1256 phosphoproteins were identified with a false-discovery rate of ~1% in phosphopeptide level (Fig. 1*A*, supplemental Table S1).

The quantitative analysis revealed 200, 69, 3, and 40 phosphopeptides that were significantly differentially abundant comparing infected and control (mock) cells at 0, 1, 2, or 4 h, respectively (Fig. 1*B* and supplemental Fig. S1, supplemental Tables S2–S5). To provide insights on the kinase families activated or repressed during *Francisella* infection, specific kinase motifs were searched. Although protein kinase motifs are often redundant, it is possible to assign these sequences

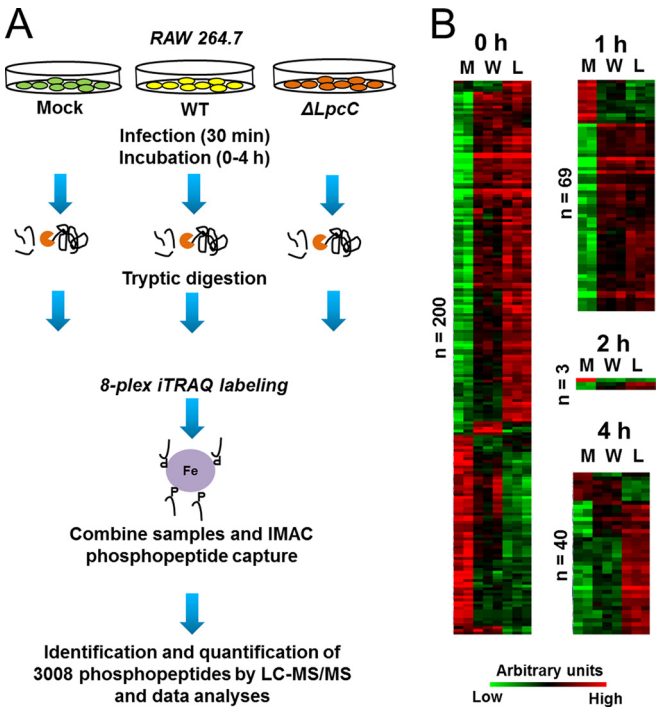

FIG. 1. **Phosphoproteome analysis of cells infected with *F. novicida*.** *A*, Experimental design. RAW 264.7 macrophage-like cells were infected for 30 min with wild-type (WT) *Francisella* or with Δ*lpcC*, followed by incubation for 0–4 h before harvesting. A negative control was run in parallel using media alone (Mock). After infection, cells were harvested, digested with trypsin and the resulting peptides were labeled with iTRAQ. Equal parts of each iTRAQ sample were combined and phosphopeptides were captured by immobilized metal affinity chromatography (IMAC). Enriched phosphopeptide fractions were analyzed by liquid chromatography-tandem mass spectrometry (LC-MS/MS) leading to the identification of 3008 phosphopeptides. *B*, Differentially abundant phosphopeptides from RAW 264.7 cells after *Francisella* infection. Abbreviations: L, Δ*lpcC*-infected; M, mock-infected; n, number of phosphopeptides; W, wild type-infected.

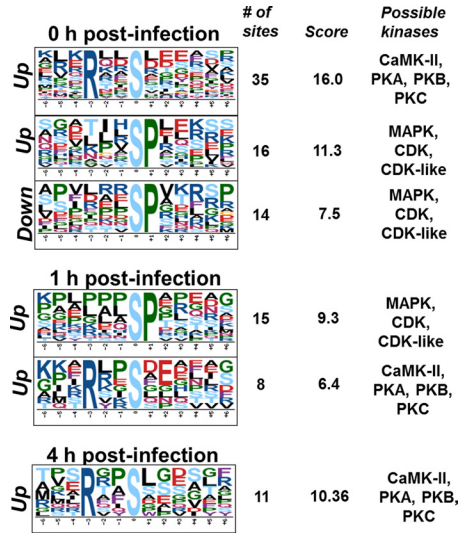

FIG. 2. **Analysis of phosphorylation motifs differentially abundant in cells infected with *F. novicida*.** Enrichment of phosphorylation site motifs was performed using Motif-x (http://motif-x.med.harvard.edu/) and only the significantly different phosphopeptides in the course of infection. Abbreviations: Up, up-regulated phosphorylation sites; Down, down-regulated phosphorylation sites.

to enzyme families, thus providing insights about classes of kinases differentially activated during the cell invasion process (48). At the early time point (0 h postinfection) two motifs (RxxS and SP, x being any amino acid residue) were found to be enriched among the up-regulated phosphorylation sites, and one motif (SP) was identified among down-regulated phosphorylation sites (Fig. 2). At 1 h postinfection, both RxxS and SP motifs were overrepresented among the up-regulated phosphorylation sites, but no overrepresented motif was found for the down-regulated sites, likely because of the low number of down-regulated phosphopeptides. At the last time point, only the RxxS motif was found to be overrepresented in the up-regulated sites (Fig. 2). The motif RxxS is consistent with either calmodulin kinase 2 (CaMK-II), PKA, PBK/AKT, or PKC, whereas SP is consistent with ERK/MAPK, CDK, and CDK-like motifs, thus suggesting that enzymes from these families might be regulated during *Francisella* infection. In agreement with these observations, *Francisella* infection is known to activate TLR2, which triggers a cascade of MAPKs (26).

To investigate potential pathways activated during *Francisella* infection, we built a protein–protein interaction (PPI) network and performed a function-enrichment analysis. For this analysis we combined differentially phosphorylated proteins found in all time points because proteins from the same pathway are not necessarily simultaneously phosphorylated. The PPI network was based on experimentally identified interactions deposited in InnateDB. To have a more insightful network, only proteins with significantly changing phosphorylation sites were used, resulting in a network of 222 proteins (nodes) and 383 connections (edges). The network showed a great number of proteins involved in transcription and translation regulation (RNA processing and post-transcription regulation), as well as degradation of polypeptides (proteasome) (Fig. 3*A*). In support of the network analysis, these functions, besides protein degradation, were found to be significantly overrepresented by a DAVID analysis (Fig. 3*B*). Interestingly, regulators of cytoskeleton organization and phagocytosis were also enriched among the differentially phosphorylated proteins (Figs. 3*A* and 3*B*), which may suggest the utilization of these pathways in the host cell entry process by the bacteria. The protein network and function-enrichment analysis were also consistent with motifs found to be overrepresented in our analysis. For instance, the motif analyses suggested that CDKs might be regulated during the infection process and, in accordance with these data, cell cycle function was suggested by the network and functional enrichment analysis to be altered during infection (Figs. 1*B*, 3*A*, and 3*B*).

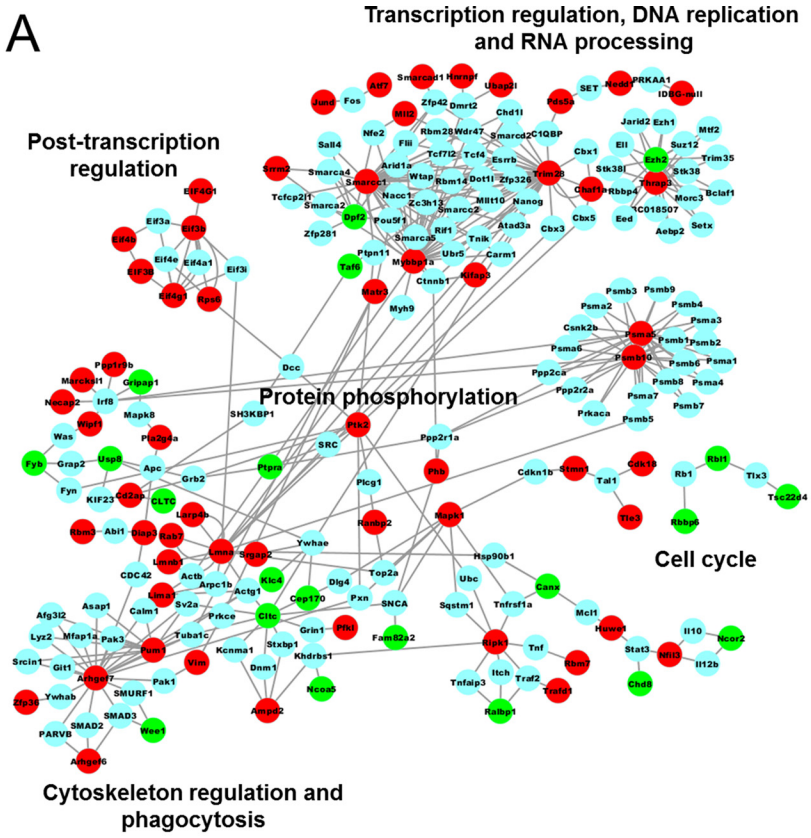

B

Functions	Count	% phosphoproteins	Enrichment (folds)	*p*-value
Cell cycle	17	9.2	2.8	3.66E-04
RNA processing	15	8.1	3.4	1.13E-04
Cytoskeleton organization	14	7.6	4.3	2.17E-05
Fc gamma R-mediated phagocytosis	6	3.2	6.6	1.81E-03
Protein phosphorylation	14	7.6	2.2	1.12E-02
DNA replication	6	3.2	3.9	1.78E-02
Regulation of transcription	34	18.4	1.5	1.01E-02
Post-transcriptional regulation of gene expression	8	4.3	5.4	6.84E-04

FIG. 3. **Analysis of functions over-represented among differentially phosphorylated proteins in *F. novicida* infection.** *A*, Network of differentially phosphorylated proteins in RAW 264.7 cells during *Francisella* infection. A protein–protein interaction map of the differentially phosphorylated proteins was retrieved from InnateDB and the network was built using Cytoscape. Circles (nodes) represent each protein and lines indicate physical interactions. Nodes were colored according to the phosphorylation abundance in infected cells compared with the mock infection: red, up-regulated; green, down-regulated; blue, either unchanged or not identified by LC-MS/MS. *B*, Enriched functions among the differentially phosphorylated proteins in RAW 264.7 cells during *Francisella* infection. Overrepresented functions were annotated using Database for Annotation, Visualization and Integrated Discovery (DAVID).

Comparative Analysis of Wild-Type Versus ΔlpcC Infected Cells—To better understand the mechanism of host cell invasion and killing by the Δ*lpcC* mutant, we investigated the differences in phosphorylation patterns between RAW 264.7 cells infected with WT or Δ*lpcC F. novicida* strains. At the earliest time point (0 h postinfection) phosphorylation signals, seemed to be stronger, but not significant, in Δ*lpcC*-infected cells compared with WT-infected cells (Fig. 1*B*). At 1 and 2 h postinfection the levels of protein phosphorylation in both Δ*lpcC*- and WT-infected cells were almost identical (Fig. 1*B*). The largest differences were observed at 4 h postinfection (Fig. 1*B*). We speculate that the signaling observed 4 h postinfection is dependent on bacterial escape from the phagosome into the host cell cytosol. Supporting this notion, the escape from the phagosome occurs from 30 min to 4 h postinfection (11). Furthermore, after the bacteria gain access to the host cell cytosol some signaling occurs, such as inflammasome activation by AIM2 (29).

To determine the significantly different phosphopeptides from WT- and Δ*lpcC*-infected cells a pairwise analysis was done using the Benjamin-Hochberg test. A total of 36 phosphopeptides were significantly different in Δ*lpcC* infection compared with WT infection and were only observed at 4 h postinfection (Fig. 4*A*, supplemental Table S6). Among the enriched motifs, the RxxS motif was enriched within the up-regulated phosphorylation sites (Fig. 4*B*), which suggests that kinases with preference to basic motifs, such as PKB/Akt, are active at this time point.

To identify pathways that were affected by proteins differentially phosphorylated between WT and Δ*lpcC* infections, we searched for overrepresented functions. Only four gene ontology categories were enriched: cell leading edge, anchoring junction, negative regulation of gene expression and RNA processing (Fig. 4*C*). Indeed cell leading edge and anchoring junction functions shared several proteins, thus we believe that indeed they reflect the same pathway of cytoskeleton

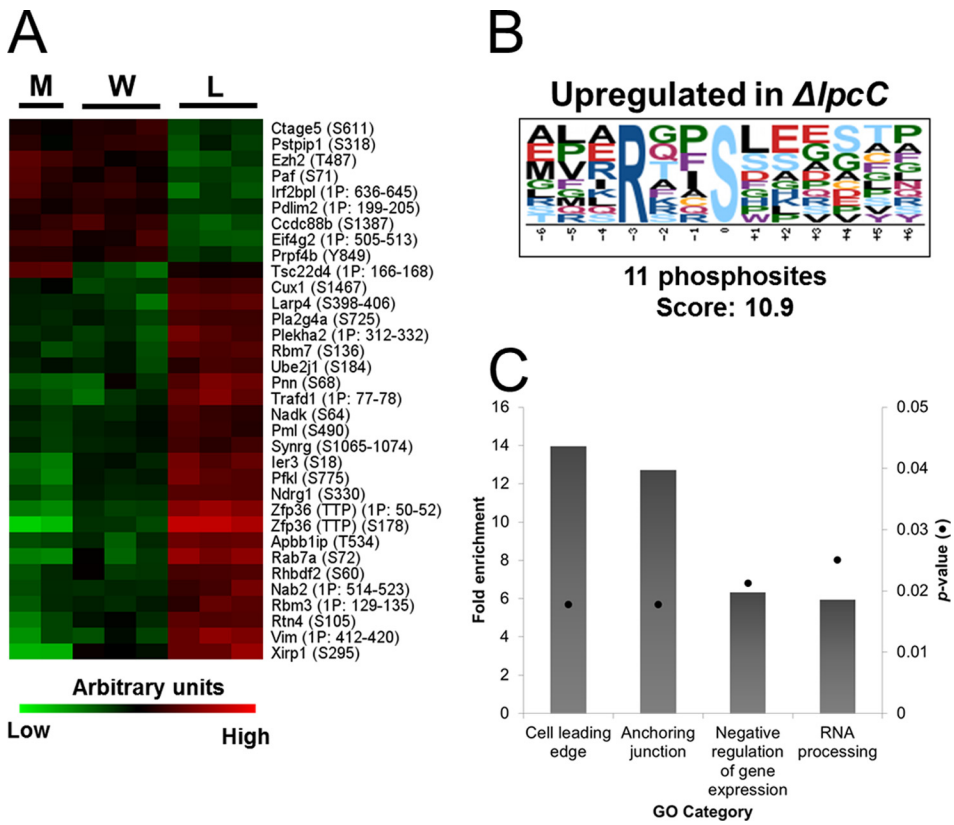

FIG. 4. **Differentially phosphorylated proteins in cells infected with wild-type (W) or Δ*lpcC* (L) *F. novicida*.** *A*, Significantly different phosphopeptides in WT or Δ*lpcC* infection. Assigned phosphorylation sites are in parentheses and sites that were not confidently assigned to a single amino acid residue (Ascore < 19.0 or -1) are represented by the number of phosphogroups and range of potential modification sites. *B*, Enriched motif among the phosphosites that were differentially abundant comparing WT and Δ*lpcC F. novicida* infection. *C*, Enriched functions among the differentially phosphorylated proteins in RAW 264.7 cells comparing infection with WT and Δ*lpcC F. novicida* strains.

rearrangement. The same was observed for negative regulation of gene expression and RNA processing, which we interpret as down-regulation of gene expression by RNA degradation. Accordingly, we next performed a more complete analysis of the proteins involved in these pathways and attempted to correlate them with Δ*lpcC* phenotypes.

Phosphorylation of Phagocytic and Cytoskeleton Proteins—To identify phosphorylation events that could be involved in the host cell invasion by Δ*lpcC*, we examined the phosphorylation quantification of proteins known to be involved in *Francisella* entry in the host cells. *Francisella* entry into host cells occurs mainly by two general mechanisms: endocytosis and phagocytosis (11, 22). In the endocytic process, *Francisella* enters host cells through cholesterol-rich domains in the plasma membrane. This process depends on clathrin and two adaptor proteins, Eps15 and AP2 (22). In the phosphoproteomic data, phosphorylation of the heavy chain of clathrin (Cltc) was shown to be reduced at the earliest time point after infection (0 h) but unchanged at the later time points (Fig. 5*A*). Cltc was also slightly less phosphorylated during the infection with the WT compared with Δ*lpcC*, but this difference was not significant (supplemental Table S2). Eps15 phosphorylation levels were unchanged over the two time points when a peptide from this protein was detected, and no phosphopeptides derived from AP2 were found. These observations suggest that the endocytic process might not be involved in the enhanced infectivity by Δ*lpcC* or that this process is not controlled by phosphorylation.

The phagocytic process of *Francisella* by host cells involves at least five receptors: MR, SRA, FcγR, CR3, and SEN (17–19). Of these known *Francisella* receptors, only phosphopeptides from FcγR were identified in our phosphoproteomic dataset, and no changes in the phosphorylation levels were observed (Fig. 5*A*). It is possible that Δ*lpcC* is more easily recognized by one or more of these receptors because of the lack of LPS polysaccharides on the cell surface. Indeed, previous work has shown the importance of LPS O antigen polysaccharide on the regulation of complement deposition on *Francisella* surface (49). The deposition of the complement protein C3 on *Francisella* surface enables the recognition of the bacteria by CR3 promoting phagocytosis by opsonization (13, 50); however, we inactivated complement proteins in our experimental conditions.

After recognizing bacteria, the phagocytic receptors trigger cell signaling that results in the rearrangement of cytoskeleton and engulfment of the particle. In the case of *Francisella*, two

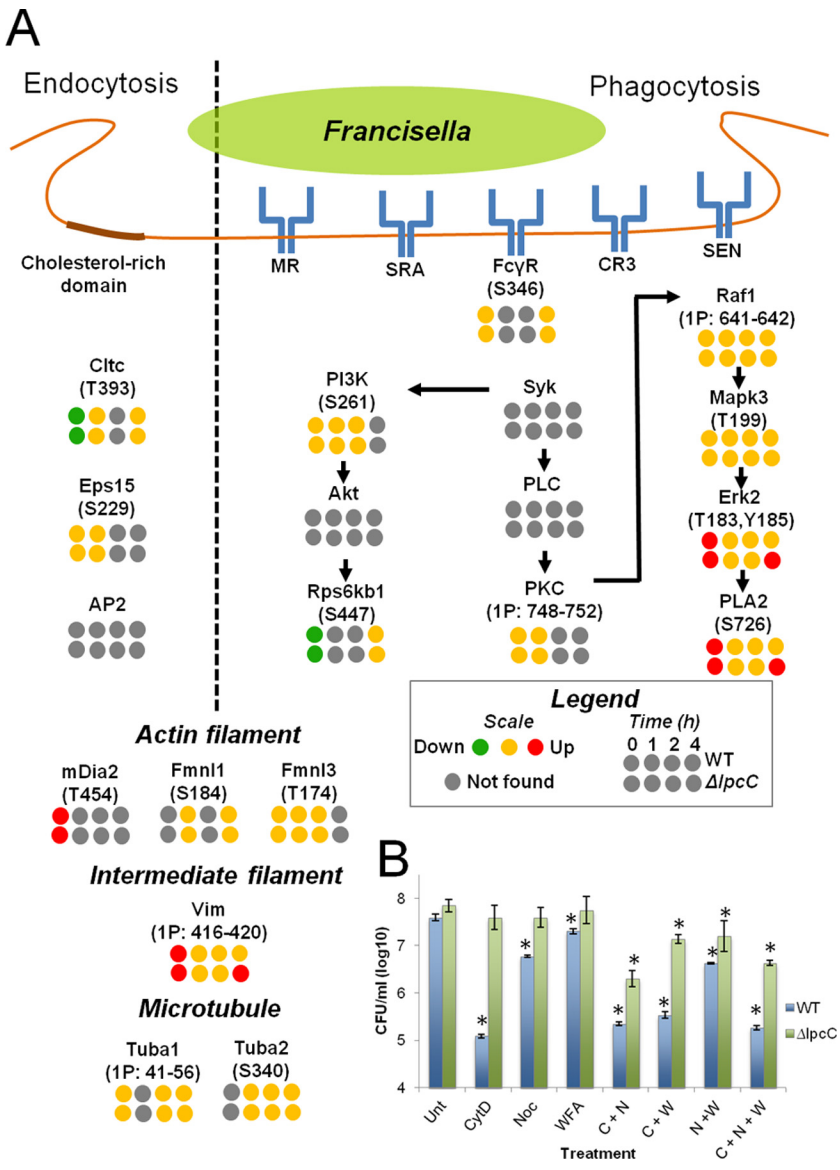

FIG. 5. **Phosphorylation on endocytic, phagocytic, and cytoskeleton proteins, and the mechanism of cell invasion.** *A*, Phosphorylation on endocytic, phagocytic and cytoskeleton proteins. The endocytic, phagocytic and cytoskeleton rearrangement pathways were built based on literature search (see text for references) and KEGG database. *B*, Contribution of cytoskeleton filaments to host cell entry of WT and Δ*lpcC F. novicida* strains. J774 cells were left untreated (Unt) or treated with 5 μg/ml cytochalasin D (CytD or C), 10 μg/ml nocodazole (Noc or N), or 5 μM withaferin A (WFA or W) before infection with WT and Δ*lpcC F. novicida* strains. Data points significantly different to the untreated control (*t* test, $p \leq 0.05$) are marked the asterisks.

pathways have been reported to be activated during the phagocytosis process: phosphoinositol 3-kinase (PI3K)/Akt and the tyrosine kinase Syk/mitogen-activated protein kinase (MAPK) Erk2 pathways (20, 21). For the PI3K/Akt pathway, phosphopeptides for PI3K and ribosomal protein S6 kinase beta-1 (Rps6kb1) were identified. Although the phosphorylation on PI3K remained unchanged, Rps6kb1 phosphorylation decreased in both WT and Δ*lpcC* infection in early time points (Fig. 5*A*). The lack of phosphorylation up-regulation suggests that this pathway was not activated during the infection. Indeed, another report has provided contradictory results regarding the role of PI3K/Akt pathway during *Francisella* phagocytosis (20), which could be potentially explained by their use of different bacterial strains. On the other hand, two proteins from the Syk/Erk2 pathway, kinase Erk2 and phospholipase A2 (PLA2), were shown to be more phosphorylated in both WT and Δ*lpcC Francisella* infection at 0 h postinfection (Fig. 5*A*). That only the last two enzymes of the cascade were found to be overphosphorylated may indicate that the upstream signaling had already faded. Interestingly, phosphorylation of these proteins was up-regulated in Δ*lpcC*-infected cells as compared with WT infection at 4 h (Fig. 5*A*), which suggests that this pathway could also be involved in the phagocytosis of Δ*lpcC*.

Next, we analyzed cytoskeletal proteins that can be involved in the engulfment of bacteria. Although more proteins involved in actin filament organization were found to be phosphorylated, only three were previously described to have a role in phagocytic or endocytic pathways: mDia2, and formin-like proteins 1 (Fmnl1) and 3 (Fmnl3) (51). Among these proteins, only phosphorylation on mDia2 was found to be up-regulated at the earliest infection time point, and no difference between WT and Δ*lpcC* infection was observed (Fig. 5*A*). Among the microtubule proteins, tubulins were found to be

phosphorylated, but their modification levels did not change with the *F. novicida* infection (Fig. 5*A*). On the other hand, the intermediate filament protein vimentin was phosphorylated in multiple sites (Table S1). Vimentin phosphorylation was higher in the early time point in both WT and Δ*lpcC* infections, but was up-regulated only in Δ*lpcC* at 4 h postinfection in a pattern that was consistent with Erk2 and PLA2 phosphorylation (Fig. 5*A*). Indeed, vimentin has previously been shown to interact with PLA2 (52); therefore, it is reasonable to believe that they could be involved in similar cellular signaling pathways. Furthermore, previous studies indicate that vimentin filaments are regulated by phosphorylation (53).

To test whether intermediate filaments and microtubules have a function in *Francisella* entry into host cells, J774 cells were treated with cytochalasin D, nocodazole and withaferin A, which are inhibitors of actin, microtubules, and intermediate (vimentin) filaments, respectively. As previously shown (34), Δ*lpcC F. novicida* infected at a higher rate compared with WT, and the inhibition of host cell actin polymerization with cytochalasin D decreased the infectivity of the WT bacteria (more than 2 logs) to a much greater extent than in the Δ*lpcC* infection (Fig. 5*B*). Blocking microtubule polymerization with nocodazole also led to a similar phenotype of decreasing bacterial entry in a greater extent in the WT (~1 log) compared with the Δ*lpcC* (not significant) infection (Fig. 5*B*). Inhibition of vimentin polymerization with withaferin A by itself had only a small effect on the entry of WT *Francisella* into the host cells, but in combination with nocodazole and cytochalasin D it significantly reduced the number of internalized bacteria (Fig. 5*B*). The individual treatments with cytochalasin D, nocodazole and withaferin A had no effect on the entry of Δ*lpcC* into host cells, but in combination these inhibitors significantly reduced the number of internalized bacteria (up to ~1 log) (Fig. 5*B*). It should be noted that the reduction in the number of internalized bacteria was smaller in Δ*lpcC* infection compared with WT for all the treatments, suggesting that whereas all these 3 cytoskeleton filaments play a role during *Francisella* infection an additional factor may be required for entry of Δ*lpcC F. novicida* uptake via the endocytic pathway.

Phosphorylation of RNA-processing Proteins, Post-transcription Regulation, and Mechanism of Cell Killing by ΔlpcC—We next performed an in-depth analysis of the proteins involved in RNA degradation, as this group was overrepresented among the differentially abundant phosphoproteins in cells infected with Δ*lpcC* compared with WT *Francisella*. The phosphoprotein tristetraprolin (TTP), product of the gene *zfp36*, drew our interest in particular because it contained two phosphopeptides with the most pronounced difference between Δ*lpcC versus* WT *Francisella* infection (Fig. 4*A*). Thus, we decided to validate TTP and investigate possible functions for differential phosphorylation during *Francisella* infection. Fig. 6*A* shows the MS/MS spectrum of a peptide corresponding to the phosphorylation at serine 178, and the magnified region details the signal intensity of the

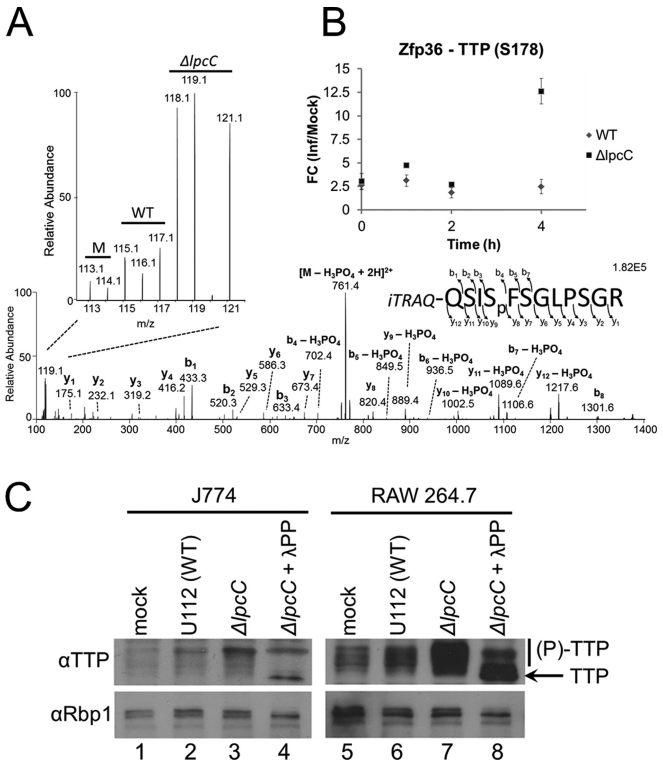

FIG. 6. **Dynamics of TTP phosphorylation in RAW 264.** 7 cells during *Francisella* infection. *A*, Tandem mass spectrum illustrating the identification and quantification of the phosphopeptide QSISpFSGLPSGR (corresponding to phosphorylation at serine 178) from tristetraprolin (Zfp36 or TTP) at 4 h postinfection. The expanded region highlights the iTRAQ report ions used for quantification. *B*, Time course quantification of TTP phosphorylation at serine 178. *C*, Western blot analysis of J774 and RAW 264.7 cell lines 4 h post infection with WT or Δ*lpcC F. novicida*. The presence of phosphorylation on TTP was determined by shift of electrophoretic mobility on treatment with λ-phosphatase (λPP).

iTRAQ report ions used for the quantitative analysis clearly shows a difference between WT and Δ*lpcC* infections. The quantification at the 4 h time point exhibited 2.5- and 12.6-fold increases in WT and Δ*lpcC Francisella* infection compared with the mock, respectively (Fig. 6*B*). This observation was further validated by Western blot analysis. In independent experiments using both J774 and RAW 264.7 macrophages, we observed a dramatic increase in the phosphorylation status of endogenous TTP, indicated by the appearance of multiple higher molecular weight bands, particularly following infection with Δ*lpcC Francisella* compared with WT (Fig. 6*C*). Importantly, these higher molecular weight bands were diminished on treatment with λ-phosphatase, consistent with a shift in electrophoretic mobility because of phosphorylation (Fig. 6*C*). The Western blot against subunit 1 of RNA Polymerase II (Rbp1) served as a loading control, as well as a positive control for the phosphatase treatment (Fig. 6*C*).

With this support for hyper-phosphorylation of TTP by phosphoproteomic and Western blot analyses, we next investigated if this phenomenon could have consequences for *in*

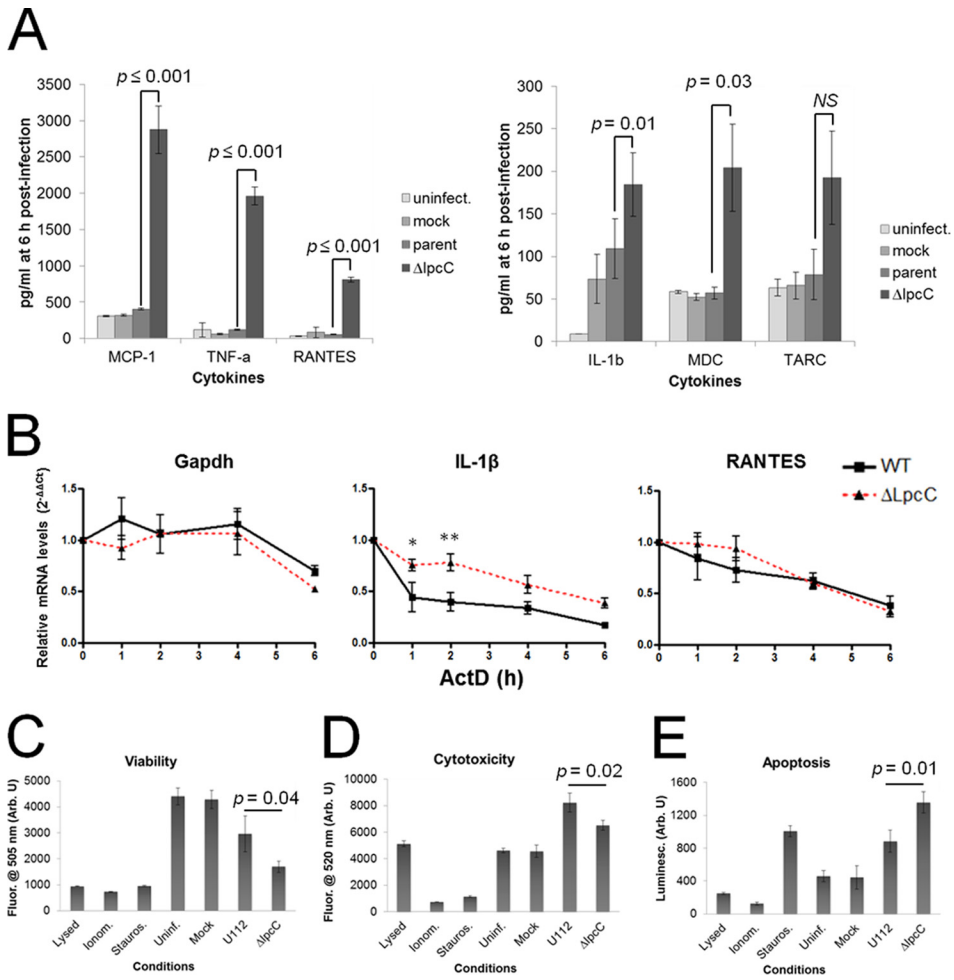

FIG. 7. **Cytokine profile and killing mechanism of cells infected with *F. novicida*.** *A*, Cytokine profile. Cytokines were measured in culture supernatants 6 h postinfection using the Q-Plex Array™ kit. *B*, mRNA stability for IL-1β and RANTES was determined with qPCR following infection and Actinomycin D treatment. ($n = 3$, $\pm$S.E., 2-way ANOVA, $p < 0.001$ for IL-1β, Bonferroni post tests, $^{*}p < 0.05$, $^{**}p < 0.01$) Viability (*C*), cytotoxicity (*D*), and apoptosis/necrosis (*E*) assays. Cells were infected with WT and Δ*lpcC F. novicida* strains and assayed for viability, cytotoxicity and apoptosis/necrosis using the ApoTox-Glo™ Triplex Assay kit. As positive controls for lysis, necrosis and apoptosis, cells were treated with saponin, ionomycin (Ionom.), staurosporine (Stauros.), respectively.

vivo murine infections. TTP is a well-known component of the mRNA-destabilizing machinery that binds to AU-rich elements (54, 55). TTP is also known to be hyper-phosphorylated by p38 MAPK, which is associated with a decrease in the RNA-binding capacity of this protein and results in the subsequent inhibition of RNA degradation (55, 56). In addition, as a negative feedback mechanism TTP phosphorylation was shown to be regulated by protein phosphatase 2A (57). Because TTP hyper-phosphorylation was observed with a much higher intensity in the Δ*lpcC* infection ($p < 0.01$), we hypothesized that *Francisella* could be down regulating TTP phosphorylation as a mechanism to shut down the translation of important factors that control its infection. To test this hypothesis we performed transcriptomic analyses using spleens of mice infected with either Δ*lpcC* or WT *Francisella*. We measured the abundance of ~30,000 genes by microarray, which showed a more drastic change in expression profiles in mice infected with WT compared with Δ*lpcC Francisella* (supplemental Fig. S2*A*, supplemental Table S7). Next, we investigated the levels of transcripts that were recently identified as TTP substrates (54). Out of 310 mRNAs identified as targets of TTP, 245 were present in our dataset (supplemental Figs. S2*B* and S2*C*, supplemental Table S8). Although the TTP-regulated RNAs were on average slightly more abundant in Δ*lpcC*-infected samples compared with mock infections, they were slightly reduced in WT infections (supplemental Figs. S2*B* and S2*C*). To test if this difference in transcript abundance among the TTP-regulated RNAs was significant, we compared the transcripts found during Δ*lpcC* infections to those observed in WT infections (*t* test, $p \leq 0.05$). Although 25% of the transcripts were more abundant in Δ*lpcC* compared with WT infections, this proportion was increased to 45% when only the TTP-regulated RNAs were considered, showing a clear enrichment (Chi-square contingency test, $p = 0.0001$). These

data suggest that hyper-phosphorylation on TTP has an impact on the transcript levels during *Francisella* infection. These results may help explain the down-regulation of many immune response genes observed in monocytes infected with either *F. novicida* or *F. tularensis* Schu S4 (58).

TTP has been shown to be a key player on the regulation of cytokine production (54, 55, 59). Thus, we speculate that *Francisella* may inhibit TTP phosphorylation and consequently targeting the mRNA of selected cytokines to degradation and preventing their translation. To test this hypothesis, we infected RAW 264.7 cells and measured the cytokines by a multiplex ELISA array 6 h after infection. Six cytokines were shown to be produced in higher amounts during infection with Δ*lpcC* compared with WT: IL-1β, MDC, TARC, MCP-1, TNF-α and RANTES (Fig. 7*A*). Out of these six, IL-1β, MDC, MCP-1 and TNF-α, have been previously shown to be regulated by TTP. These results suggest that *Francisella* impairs the production of cytokines, likely by a mechanism that involves TTP-mediated mRNA degradation. To directly investigate this mechanism in RAW 264.7 cells, we used qPCR to monitor mRNA stability of IL-1β and RANTES cytokines after infection and in the presence of actinomycin D (Fig. 7*B*). IL-1β and RANTES were selected as representative pro-inflammatory cytokines and chemokines, respectively. With IL-1β, we observed a deficiency in its mRNA degradation following infection with Δ*lpcC* compared with WT; the most dramatic delineation appeared within the first hour. With RANTES, there was a trending delay in mRNA degradation with Δ*lpcC* within the first 2 h but it caught up with WT by 4 h postinfection. Importantly, there were no statistically significant differences in control Gapdh mRNA stability between WT and Δ*lpcC* infection. Together, our data suggest that *Francisella* can regulate the mRNA stability of particular cytokines, such as IL-1β, but for others it may only represent a contributing mechanism.

Considering that several cytokines have cytotoxic effects, we analyzed the relationship of cytokine production and the hyper-cytotoxic phenotype of the Δ*lpcC* mutant. Because some of these cytokines, such as IL-1β and TNF-α, kill cells by triggering apoptosis (60, 61), we aimed to identify the mechanism of host cell death by Δ*lpcC* using the ApoTox-Glo™ triplex assay, which analyzes viability, necrosis, and apoptosis with the same assay well. Consistent with previous results (34), Δ*lpcC* is more cytotoxic to host cells than WT (Fig. 7*C*). Furthermore, Δ*lpcC* infection led to an increase in apoptosis, similar to the positive control with the apoptotic inducer staurosporine (Figs. 7*D* and 7*E*). These results suggest that *Francisella* avoids triggering the host apoptotic pathway potentially by inhibiting the production of select cytokines. In support of our results, *Francisella* has been shown to inhibit apoptotic signaling and to prolong the lifespan of infected neutrophils (62). Indeed, *Francisella* targeting of IL-1β- and TNF-α-mediated signaling has been proposed as potential mechanisms for anti-apoptotic activity in infected neutrophils (63).

CONCLUSIONS

We performed a comparative phosphoproteomic analysis of murine cells infected with *F. novicida*. Our data showed the participation of different cytoskeleton filaments in the process of bacterial entry into the host cells. Furthermore, by a combination of phosphoproteomics, transcriptomics, and cellular and immunological assays, we showed a deregulation of the signaling that controls TTP activity, a key component of post-transcriptional regulation in innate immune response (54, 57, 59). These findings suggest that *Francisella* targets host post-transcriptional regulatory machinery to repress the expression of innate immune factors that controls the infection.

Acknowledgments—We thank our colleagues Charles Ansong, Therese Clauss, Ron Moore, Penny Colton, and Brooke Kaiser for insightful comments, input, and suggestions.

* This work was supported by the National Institute of Allergy and Infectious Diseases (NIH/DHHS through interagency agreement Y1-AI-4894-01; project website www.SysBEP.org) and the National Institute for General Medicine (GM094623). This work used instrumentation and capabilities developed with support from the NIH grant 5P41RR018522-10, the National Institute of General Medical Sciences grant 8 P41 GM103493-10, and the U. S. Department of Energy Office of Biological and Environmental Research (DOE/BER). Significant portions of this work were performed in the EMSL, a DOE/BER national scientific user facility located at Pacific Northwest National Laboratory. The Pacific Northwest National Laboratory is operated for the DOE by Battelle under Contract DE-AC05-76RLO1830. This work was also supported by the NIH award NS076094 to X.A.C.

S This article contains supplemental Figs. S1 and S2 and Tables S1 to S8.

** To whom correspondence should be addressed: Department of Molecular Microbiology and Immunology, L220, Oregon Health and Science University, 3181 SW Sam Jackson Park Road, Portland, OR 97239. Tel.: (503) 494-6841; Fax: (503) 494-6862; E-mail: tempelr@ohsu.edu.

‡‡Current address: Bindley Bioscience Center, Purdue University, West Lafayette, IN, USA.

§§Both authors contributed equally to this work.

Data availability: The LC-MS/MS runs and annotated spectra are available at PeptideAtlas under the accession number PASS00297.

REFERENCES

1. Sjostedt, A. (2007) Tularemia: history, epidemiology, pathogen physiology, and clinical manifestations. *Ann. N. Y. Acad. Sci.* **1105,** 1–29
2. Sjostedt, A. (2005) Family III. *Francisellaceae.* in *Bergey's Manual® of Systematic Bacteriology* (Brenner, D. J., Krieg, N. R., Staley, J. T., and Garrity, G. M. eds.), Springer, New York, NY. pp 199–209
3. Champion, M. D., Zeng, Q., Nix, E. B., Nano, F. E., Keim, P., Kodira, C. D., Borowsky, M., Young, S., Koehrsen, M., Engels, R., Pearson, M., Howarth, C., Larson, L., White, J., Alvarado, L., Forsman, M., Bearden, S. W., Sjostedt, A., Titball, R., Michell, S. L., Birren, B., and Galagan, J. (2009) Comparative genomic characterization of Francisella tularensis strains belonging to low and high virulence subspecies. *PLoS Pathogens* **5,** e1000459
4. Rohmer, L., Fong, C., Abmayr, S., Wasnick, M., Larson Freeman, T. J., Radey, M., Guina, T., Svensson, K., Hayden, H. S., Jacobs, M., Gallagher, L. A., Manoil, C., Ernst, R. K., Drees, B., Buckley, D., Haugen, E., Bovee, D., Zhou, Y., Chang, J., Levy, R., Lim, R., Gillett, W., Guenthener,

D., Kang, A., Shaffer, S. A., Taylor, G., Chen, J., Gallis, B., D'Argenio, D. A., Forsman, M., Olson, M. V., Goodlett, D. R., Kaul, R., Miller, S. I., and Brittnacher, M. J. (2007) Comparison of Francisella tularensis genomes reveals evolutionary events associated with the emergence of human pathogenic strains. *Genome Biol.* **8,** R102

5. Thomas, R. M., Titball, R. W., Oyston, P. C., Griffin, K., Waters, E., Hitchen, P. G., Michell, S. L., Grice, I. D., Wilson, J. C., and Prior, J. L. (2007) The immunologically distinct O antigens from Francisella tularensis subspecies tularensis and Francisella novicida are both virulence determinants and protective antigens. *Infection Immunity* **75,** 371–378
6. Atianand, M. K., Duffy, E. B., Shah, A., Kar, S., Malik, M., and Harton, J. A. (2011) Francisella tularensis reveals a disparity between human and mouse NLRP3 inflammasome activation. *J. Biol. Chem.* **286,** 39033–39042
7. Dotson, R. J., Rabadi, S. M., Westcott, E. L., Bradley, S., Catlett, S. V., Banik, S., Harton, J. A., Bakshi, C. S., and Malik, M. (2013) Repression of inflammasome by Francisella tularensis during early stages of infection. *J. Biol. Chem. in press* **288,** 23844–23857
8. Shen, H., Chen, W., and Conlan, J. W. (2004) Mice sublethally infected with Francisella novicida U112 develop only marginal protective immunity against systemic or aerosol challenge with virulent type A or B strains of F. tularensis. *Microb. Pathogenesis* **37,** 107–110
9. Asare, R., and Kwaik, Y. A. (2010) Exploitation of host cell biology and evasion of immunity by francisella tularensis. *Front. Microbiol.* **1,** 145
10. Henry, T., and Monack, D. M. (2007) Activation of the inflammasome upon Francisella tularensis infection: interplay of innate immune pathways and virulence factors. *Cell. Microbiol.* **9,** 2543–2551
11. Jones, C. L., Napier, B. A., Sampson, T. R., Llewellyn, A. C., Schroeder, M. R., and Weiss, D. S. (2012) Subversion of host recognition and defense systems by Francisella spp. *Microbiol. Mol. Biol. Rev.* **76,** 383–404
12. Bosio, C. M. (2011) The subversion of the immune system by francisella tularensis. *Front. Microbiol.* **2,** 9
13. Balagopal, A., MacFarlane, A. S., Mohapatra, N., Soni, S., Gunn, J. S., and Schlesinger, L. S. (2006) Characterization of the receptor-ligand pathways important for entry and survival of Francisella tularensis in human macrophages. *Infection Immunity* **74,** 5114–5125
14. Barel, M., Hovanessian, A. G., Meibom, K., Briand, J. P., Dupuis, M., and Charbit, A. (2008) A novel receptor - ligand pathway for entry of Francisella tularensis in monocyte-like THP-1 cells: interaction between surface nucleolin and bacterial elongation factor Tu. *BMC Microbiol.* **8,** 145
15. Geier, H., and Celli, J. (2011) Phagocytic receptors dictate phagosomal escape and intracellular proliferation of Francisella tularensis. *Infection Immunity* **79,** 2204–2214
16. Schulert, G. S., and Allen, L. A. (2006) Differential infection of mononuclear phagocytes by Francisella tularensis: role of the macrophage mannose receptor. *J. Leukocyte Biol.* **80,** 563–571
17. Clemens, D. L., Lee, B. Y., and Horwitz, M. A. (2005) Francisella tularensis enters macrophages via a novel process involving pseudopod loops. *Infection Immunity* **73,** 5892–5902
18. Lai, X. H., Golovliov, I., and Sjostedt, A. (2001) Francisella tularensis induces cytopathogenicity and apoptosis in murine macrophages via a mechanism that requires intracellular bacterial multiplication. *Infection Immunity* **69,** 4691–4694
19. Lindemann, S. R., McLendon, M. K., Apicella, M. A., and Jones, B. D. (2007) An in vitro model system used to study adherence and invasion of Francisella tularensis live vaccine strain in nonphagocytic cells. *Infection Immunity* **75,** 3178–3182
20. Parsa, K. V., Butchar, J. P., Rajaram, M. V., Cremer, T. J., and Tridandapani, S. (2008) The tyrosine kinase Syk promotes phagocytosis of Francisella through the activation of Erk. *Mol. Immunol.* **45,** 3012–3021
21. Tamilselvam, B., and Daefler, S. (2008) Francisella targets cholesterol-rich host cell membrane domains for entry into macrophages. *J. Immunol.* **180,** 8262–8271
22. Law, H. T., Lin, A. E. J., Kim, Y., Quach, B., Nano, F. E., and Guttman, J. A. (2011) Francisella tularensis uses cholesterol and clathrin-based endocytic mechanisms to invade hepatocytes. *Sci Rep-Uk* **1**
23. Cremer, T. J., Butchar, J. P., and Tridandapani, S. (2011) Francisella subverts innate immune signaling: Focus On PI3K/Akt. *Front. Microbiol.* **5,** 13
24. Hajjar, A. M., Harvey, M. D., Shaffer, S. A., Goodlett, D. R., Sjostedt, A., Edebro, H., Forsman, M., Bystrom, M., Pelletier, M., Wilson, C. B., Miller, S. I., Skerrett, S. J., and Ernst, R. K. (2006) Lack of in vitro and in vivo recognition of Francisella tularensis subspecies lipopolysaccharide by Toll-like receptors. *Infection Immunity* **74,** 6730–6738
25. Katz, J., Zhang, P., Martin, M., Vogel, S. N., and Michalek, S. M. (2006) Toll-like receptor 2 is required for inflammatory responses to Francisella tularensis LVS. *Infection Immunity* **74,** 2809–2816
26. Cole, L. E., Shirey, K. A., Barry, E., Santiago, A., Rallabhandi, P., Elkins, K. L., Puche, A. C., Michalek, S. M., and Vogel, S. N. (2007) Toll-like receptor 2-mediated signaling requirements for Francisella tularensis live vaccine strain infection of murine macrophages. *Infection Immunity* **75,** 4127–4137
27. Kawai, T., and Akira, S. (2011) Toll-like receptors and their crosstalk with other innate receptors in infection and immunity. *Immunity* **34,** 637–650
28. Belhocine, K., and Monack, D. M. (2012) Francisella infection triggers activation of the AIM2 inflammasome in murine dendritic cells. *Cell. Microbiol.* **14,** 71–80
29. Peng, K., Broz, P., Jones, J., Joubert, L. M., and Monack, D. (2011) Elevated AIM2-mediated pyroptosis triggered by hypercytotoxic Francisella mutant strains is attributed to increased intracellular bacteriolysis. *Cell. Microbiol.* **13,** 1586–1600
30. Jones, J. W., Kayagaki, N., Broz, P., Henry, T., Newton, K., O'Rourke, K., Chan, S., Dong, J., Qu, Y., Roose-Girma, M., Dixit, V. M., and Monack, D. M. (2010) Absent in melanoma 2 is required for innate immune recognition of Francisella tularensis. *Proc. Natl. Acad. Sci. U. S. A.***107,** 9771–9776
31. Fernandes-Alnemri, T., Yu, J. W., Juliana, C., Solorzano, L., Kang, S., Wu, J., Datta, P., McCormick, M., Huang, L., McDermott, E., Eisenlohr, L., Landel, C. P., and Alnemri, E. S. (2010) The AIM2 inflammasome is critical for innate immunity to Francisella tularensis. *Nat. Immunol.* **11,** 385–393
32. Rathinam, V. A., Jiang, Z., Waggoner, S. N., Sharma, S., Cole, L. E., Waggoner, L., Vanaja, S. K., Monks, B. G., Ganesan, S., Latz, E., Hornung, V., Vogel, S. N., Szomolanyi-Tsuda, E., and Fitzgerald, K. A. (2010) The AIM2 inflammasome is essential for host defense against cytosolic bacteria and DNA viruses. *Nat. Immunol.* **11,** 395–402
33. Broz, P., von Moltke, J., Jones, J. W., Vance, R. E., and Monack, D. M. (2010) Differential requirement for Caspase-1 autoproteolysis in pathogen-induced cell death and cytokine processing. *Cell Host Microbe* **8,** 471–483
34. Lai, X. H., Shirley, R. L., Crosa, L., Kanistanon, D., Tempel, R., Ernst, R. K., Gallagher, L. A., Manoil, C., and Heffron, F. (2010) Mutations of Francisella novicida that alter the mechanism of its phagocytosis by murine macrophages. *PloS One* **5,** e11857
35. Craven, R. R., Hall, J. D., Fuller, J. R., Taft-Benz, S., and Kawula, T. H. (2008) Francisella tularensis invasion of lung epithelial cells. *Infection Immunity* **76,** 2833–2842
36. Nguyen, T. H., Brechenmacher, L., Aldrich, J. T., Clauss, T. R., Gritsenko, M. A., Hixson, K. K., Libault, M., Tanaka, K., Yang, F., Yao, Q., Pasa-Tolic, L., Xu, D., Nguyen, H. T., and Stacey, G. (2012) Quantitative Phosphoproteomic Analysis of Soybean Root Hairs Inoculated with Bradyrhizobium japonicum. *Mol. Cell. Proteomics* **11,** 1140–1155
37. Zhao, R., Ding, S. J., Shen, Y., Camp, D. G., 2nd, Livesay, E. A., Udseth, H., and Smith, R. D. (2009) Automated metal-free multiple-column nanoLC for improved phosphopeptide analysis sensitivity and throughput. *J. Chromatog.* **877,** 663–670
38. Mayampurath, A. M., Jaitly, N., Purvine, S. O., Monroe, M. E., Auberry, K. J., Adkins, J. N., and Smith, R. D. (2008) DeconMSn: a software tool for accurate parent ion monoisotopic mass determination for tandem mass spectra. *Bioinformatics* **24,** 1021–1023
39. Kim, S., Gupta, N., and Pevzner, P. A. (2008) Spectral probabilities and generating functions of tandem mass spectra: a strike against decoy databases. *J. Proteome Res.* **7,** 3354–3363
40. Beausoleil, S. A., Villen, J., Gerber, S. A., Rush, J., and Gygi, S. P. (2006) A probability-based approach for high-throughput protein phosphorylation analysis and site localization. *Nat. Biotechnol.* **24,** 1285–1292
41. Monroe, M. E., Shaw, J. L., Daly, D. S., Adkins, J. N., and Smith, R. D. (2008) MASIC: a software program for fast quantitation and flexible visualization of chromatographic profiles from detected LC-MS(/MS) features. *Comput. Biol. Chem.* **32,** 215–217
42. Troyanskaya, O., Cantor, M., Sherlock, G., Brown, P., Hastie, T., Tibshirani,

R., Botstein, D., and Altman, R. B. (2001) Missing value estimation methods for DNA microarrays. *Bioinformatics* **17,** 520–525
43. Smyth, G. K. (2005) Limma: linear models for microarray data. in *Bioinformatics and Computational Biology Solutions using R and Bioconductor* (Gentleman, R., Carey, V., Dudoit, S., Irizarry, R., and Huber, W. eds.), Springer, New York, NY. pp 397–420
44. Schwartz, D., and Gygi, S. P. (2005) An iterative statistical approach to the identification of protein phosphorylation motifs from large-scale data sets. *Nat. Biotechnol.* **23,** 1391–1398
45. Lynn, D. J., Winsor, G. L., Chan, C., Richard, N., Laird, M. R., Barsky, A., Gardy, J. L., Roche, F. M., Chan, T. H., Shah, N., Lo, R., Naseer, M., Que, J., Yau, M., Acab, M., Tulpan, D., Whiteside, M. D., Chikatamarla, A., Mah, B., Munzner, T., Hokamp, K., Hancock, R. E., and Brinkman, F. S. (2008) InnateDB: facilitating systems-level analyses of the mammalian innate immune response. *Mol. Sys. Biol.* **4,** 218
46. Smoot, M. E., Ono, K., Ruscheinski, J., Wang, P. L., and Ideker, T. (2011) Cytoscape 2.8: new features for data integration and network visualization. *Bioinformatics* **27,** 431–432
47. Huang da, W., Sherman, B. T., and Lempicki, R. A. (2009) Systematic and integrative analysis of large gene lists using DAVID bioinformatics resources. *Nature protocols* **4,** 44–57
48. Trost, M., English, L., Lemieux, S., Courcelles, M., Desjardins, M., and Thibault, P. (2009) The phagosomal proteome in interferon-gamma-activated macrophages. *Immunity* **30,** 143–154
49. Clay, C. D., Soni, S., Gunn, J. S., and Schlesinger, L. S. (2008) Evasion of complement-mediated lysis and complement C3 deposition are regulated by Francisella tularensis lipopolysaccharide O antigen. *Journal of immunology* **181,** 5568–5578
50. Schwartz, J. T., Barker, J. H., Long, M. E., Kaufman, J., McCracken, J., and Allen, L. A. (2012) Natural IgM mediates complement-dependent uptake of Francisella tularensis by human neutrophils via complement receptors 1 and 3 in nonimmune serum. *J. Immunol.* **189,** 3064–3077
51. Campellone, K. G., and Welch, M. D. (2010) A nucleator arms race: cellular control of actin assembly. *Nat. Rev.* **11,** 237–251
52. Kuwata, H., Yamamoto, S., Miyazaki, Y., Shimbara, S., Nakatani, Y., Suzuki, H., Ueda, N., Yamamoto, S., Murakami, M., and Kudo, I. (2000) Studies on a mechanism by which cytosolic phospholipase A2 regulates the expression and function of type IIA secretory phospholipase A2. *J. Immunol.* **165,** 4024–4031
53. Eriksson, J. E., He, T., Trejo-Skalli, A. V., Harmala-Brasken, A. S., Hellman, J., Chou, Y. H., and Goldman, R. D. (2004) Specific in vivo phosphorylation sites determine the assembly dynamics of vimentin intermediate filaments. *J. Cell Sci.* **117,** 919–932
54. Kratochvill, F., Machacek, C., Vogl, C., Ebner, F., Sedlyarov, V., Gruber, A. R., Hartweger, H., Vielnascher, R., Karaghiosoff, M., Rulicke, T., Muller, M., Hofacker, I., Lang, R., and Kovarik, P. (2011) Tristetraprolin-driven regulatory circuit controls quality and timing of mRNA decay in inflammation. *Mol. Sys. Biol.* **7,** 560
55. Ronkina, N., Menon, M. B., Schwermann, J., Tiedje, C., Hitti, E., Kotlyarov, A., and Gaestel, M. (2010) MAPKAP kinases MK2 and MK3 in inflammation: complex regulation of TNF biosynthesis via expression and phosphorylation of tristetraprolin. *Biochem. Pharmacol.* **80,** 1915–1920
56. Brooks, S. A., and Blackshear, P. J. (2013) Tristetraprolin (TTP): interactions with mRNA and proteins, and current thoughts on mechanisms of action. *Biochim. Biophys. Acta* **1829,** 666–679
57. Sun, L., Stoecklin, G., Van Way, S., Hinkovska-Galcheva, V., Guo, R. F., Anderson, P., and Shanley, T. P. (2007) Tristetraprolin (TTP)-14-3-3 complex formation protects TTP from dephosphorylation by protein phosphatase 2a and stabilizes tumor necrosis factor-alpha mRNA. *J. Biol. Chem.* **282,** 3766–3777
58. Butchar, J. P., Cremer, T. J., Clay, C. D., Gavrilin, M. A., Wewers, M. D., Marsh, C. B., Schlesinger, L. S., and Tridandapani, S. (2008) Microarray analysis of human monocytes infected with Francisella tularensis identifies new targets of host response subversion. *PloS One* **3,** e2924
59. Qiu, L. Q., Stumpo, D. J., and Blackshear, P. J. (2012) Myeloid-specific tristetraprolin deficiency in mice results in extreme lipopolysaccharide sensitivity in an otherwise minimal phenotype. *J. Immunol.* **188,** 5150–5159
60. Hogquist, K. A., Nett, M. A., Unanue, E. R., and Chaplin, D. D. (1991) Interleukin 1 is processed and released during apoptosis. *Proc. Natl. Acad. Sci. U. S. A.* **88,** 8485–8489
61. Rath, P. C., and Aggarwal, B. B. (1999) TNF-induced signaling in apoptosis. *J. Clin. Immunol.* **19,** 350–364
62. Schwartz, J. T., Barker, J. H., Kaufman, J., Fayram, D. C., McCracken, J. M., and Allen, L. A. (2012) Francisella tularensis inhibits the intrinsic and extrinsic pathways to delay constitutive apoptosis and prolong human neutrophil lifespan. *J. Immunol.* **188,** 3351–3363
63. Schwartz, J. T., Bandyopadhyay, S., Kobayashi, S. D., McCracken, J., Whitney, A. R., Deleo, F. R., and Allen, L. A. (2013) Francisella tularensis alters human neutrophil gene expression: insights into the molecular basis of delayed neutrophil apoptosis. *J. Innate Immun.* **5,** 124–136